Dissertation - II

Report on

STRUCTURAL AND SPECTROSCOPIC STUDIES OF Eu^{3+} ACTIVATED POTASSIUM BISMUTH MOLYBDATE PHOSPHOR FOR OPTOELECTRONIC DEVICE APPLICATIONS

submitted towards the partial

fulfilment of the requirements for the

award of the degree of

Master of Science

in

Physics

Submitted by

DIVYANSHI NAGPAL (2K20/MSCPHY/07)

TANISHA BHADAURIA (2K20/MSCPHY/30)

Under the supervision

of

Dr. M. Jayasimhadri

Department of Applied Physics
DELHI TECHNOLOGICAL UNIVERSITY
(Formerly Delhi College of Engineering)
Bawana Road, Delhi-110042

May 2022

CANDIDATE'S DECLARATION

I hereby certify that the work, which is presented in the Dissertation-II entitled "**Structural and spectroscopic studies of Eu^{3+} activated potassium bismuth molybdate phosphor for optoelectronic device applications**" in fulfilment of the requirement for the award of the Degree of Master in Science in Physics and submitted to the Department of Applied Physics, Delhi Technological University, Delhi is an authentic record of our own, carried out during a period from January 2022 to May 2022, under the supervision of **Dr. M. Jayasimhadri**.

The work presented in this report has not been submitted and not under consideration for the award for any other course/degree of this or any other Institute/University. The work has been communicated in peer reviewed Scopus indexed conference & journal with the following details:

Title of the Paper (I): Structural and spectroscopic studies of Eu^{3+} activated potassium bismuth molybdate phosphor for optoelectronic device applications

Author names (in sequence as per research paper): Divyanshi Nagpal, Tanisha Bhadauria & M. Jayasimhadri

Name of Conference: International Conference on Materials Processing and Characterization (ICMPC)

Name of the Journal: Materials Today Proceedings, Scopus Indexed publication of Elsevier

Conference Dates with venue: April 22-24, Online, Virtual mode

Have you registered for the conference? : Yes

Status of paper (Accepted/Published/Communicated): Published

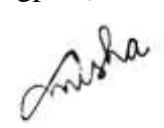**Date of paper communication:** March 31, 2022

Date of paper acceptance: April 7, 2022

Date of paper publication: May 2, 2022

Place: Delhi

Divyanshi Nagpal (2K20MSCPHY/07)

Date: 10/05/2022

Tanisha Bhadauria (2K20/MSCPHY/30)

1

DELHI TECHNOLOGICAL UNIVERSITY

(FORMERLY Delhi College of Engineering)

Bawana Road, Delhi-110042

CERTIFICATE

I hereby certify that the project Dissertation titled "Structural and spectroscopic studies of Eu^{3+} activated potassium bismuth molybdate phosphor for optoelectronic device applications" which is submitted by DIVYANSHI NAGPAL (2K20/MSCPHY/07), TANISHA BHADAURIA, (2K20/MSCPHY/30) [Masters in Physics], Delhi Technological University, Delhi in complete fulfillment of the requirement for the award of the degree of the Bachelor of Technology, is a record of the project work carried out by the students under my supervision. To the best of my knowledge this work has not been submitted in part or full for any Degree or Diploma to this University or elsewhere.

Place: Delhi

Dr. M. Jayasimhadri

(Assistant Professor)

Date: 10/05/2022

SUPERVISOR

ACKNOWLEDGEMENTS

ABSTRACT

Red emitting Eu^{3+} activated $K_5BiMo_4O_{16}$ (KBM: Eu^{3+}) phosphor has been synthesized via high temperature solid state reaction route and explored via investigating various structural and spectroscopic properties. The phase purity of the as-synthesized KBM samples have been analysed through X-ray diffraction technique. Morphological properties have been analysed through SEM images and the vibration modes have been identified in KBM crystal using Fourier Transform Infrared (FT-IR) spectroscopy. The luminescence spectrum of KBM: Eu^{3+} phosphor indicates the characteristic peaks of Eu^{3+} positioned at 578, 588, 612, 657 and 704 nm under 392 and 464 nm excitation wavelength. The color coordinates of KBM: Eu^{3+} phosphor excited with 392 and 464 nm wavelength are (0.657, 0.342) and (0.655, 0.344) located in red region. Based on the above-mentioned characteristics, KBM: Eu^{3+} phosphor may be a potential candidate to utilize in optoelectronic applications such wLEDs and solar cells.

CONTENTS

LIST OF TABLES AND FIGURES

LIST OF ABBREVIATIONS

LED	-	Light-emitting diode
w-LED	-	White Light Emitting Diode
RE	-	Rare Earth (Metals)
CCT	-	Correlated Color Temperature
JCPDS	-	Joint Committee on Powder Diffraction Standards
SEM	-	Scanning Electron Microscope
FWHM	-	Full Width at Half Maximum
CIE	-	Commission International De L' Eclairage
UV	-	Ultraviolet
PL	-	Photoluminescence
PLE	-	Photoluminescence Excitation
XRD	-	X-ray Diffraction

CHAPTER 1

INTRODUCTION

CHAPTER 1: INTRODUCTION

1.1 Phosphor

Phosphor have been used since the 19th century as a broad word for substances that emit light when exposed to darkness. Each phosphor does have its unique set of properties, such as emission colors and the amount of time it takes to glow just after excitation stops. Electroluminescence occurs whenever a phosphor generates light as a result of electron excitation, and all these phosphors are used to make video displays and workstation monitors. Photoluminescence is a means of stimulating phosphor with UV, visible, and infrared radiation. It is most commonly used in fluorescents for ambient illumination [1].

Fig. 1.1. Phosphor emitting light

Phosphor are divided into numerous groups according to the parameters used to classify them. We're talking about chemical phosphor here. The most common form of inorganic phosphor is a dry powder. Various synthetic procedures are used to create these powder specimens. The concept is to use a host matrix around which to dope any activator ion, such as a Rare-Earth ion. Rare-earth ions are the most often employed activator ions [2, 3].

Phosphor are made up of composites such as oxide, oxynitride, sulfide, selenide, halide, borates, and oxyhalide that are doped with minute amounts of activator ions, which could be rare-earth or transition element ions. The activator ions behave as radiation or light centers with their own energy levels, which are inhabited by stimulation or energy transfer [4, 5].

An effective phosphor will be able to utilize excitation energy while transmitting light as shown in Fig. 1.1. To avoid an afterglow, the duration between excitation and emission should be as short as possible. Energy absorption can occur at the activator ion or anywhere else in the lattice, but the energy must finally be transferred to the radiating core for emissions to occur [6]. The absorbed energy can also be lost in the form of radiation-free disintegration, lowering the quantum efficiency. Effective phosphor securely hold their ions, reducing energy loss through non-radiative transitions. Contaminant ions absorb or redirect energy, halting the material's luminous properties [7].

The color range (three emitting colors-red, green, and blue), the lumen equivalency, the emission spectrum, quantum yield, and the emission lifespan are all essential factors for phosphor materials. To get color points, the emission spectrum energy division is employed, which is computed using the Commission International de L'Eclairage (CIE) graphic rule. A higher luminosity count indicates a strong light. The lumen equivalent of a phosphor should be higher. When an atom or molecule transitions from high to low energy levels, a range of frequencies known as the emission spectrum of electromagnetic radiation is communicated. To be utilized economically, any phosphor's emission lifespan should be long. Quantum efficiency is a measure of the quantity and wavelengths of emitted photons from a phosphor if we recognize the amount of triggering photons at specific wavelengths [8]. The decaying time (afterglow or persistence) of a phosphor is defined as the time it takes for the emission intensity to drop to 10% of its initial intensity after stimulation ends. The decay time is determined by the substance's intrinsic properties [9].

Rare earths such as Tb^{3+}, Eu^{2+}, Dy^{3+}, Mn^{2+}, and Eu^{3+} are examples of d-electrons in action. The crystalline host lattice engages favorably with the d-orbit. There are a number of critical characteristics to consider when determining if the synthesized phosphor is suitable for further use. Chemical and thermal stability, quantum efficiency, color point, biodegradability, emission spectrum, and longevity are only a few of the considerations. Plasma and field-emission displays, light-emitting diodes, solar cell applications, thermal sensors, and other applications are all possible using phosphor materials [10].

1.2 Host matrix and activator ions

Phosphor are made up of a host matrix and an activator, which is a radiating core. Inorganic hosts have several features including physical, thermal, and chemical inertness, and hence serve as ideal candidates. Self-activated hosts are preferred over inorganic hosts since they produce their inherent intense and broadly visible radiation in response to UV stimulation, which is utilized by the activator to improve emission intensity [11].

The activator is a dopant that is introduced to the material's crystal to induce the desired form of inhomogeneity. The activators lengthen the time it takes for the emission to occur. The activator concentration in the crystals is also quite important. Whereas the host substance is microcrystalline and transparent to visible light, the activators absorb and emit radiation [12].

The activator gathers the stimulating radiation and amplifies it to a state of excitement. Luminescence does not occur in every ion or element. The radiation pattern, the absorption spectrum, and the proportion of the frequencies of radiative and non-radiative reversion to the ground state are the properties to be indicated by this approach. This determines the capacity of luminous compounds to convert light[13].

Liquid crystal display panels constructed of rare earth (Eu^{3+}) phosphor grab 10 times more brightness, and white LEDs built of a combination of three rare earth phosphor are 80 % more efficient than incandescent lamps for excellent energy efficiency [14].

When achieving narrow-band luminosity in the visible spectrum, rare earth elements are employed wherein light emission is a performance criterion because their electronic structure enables efficacy throughout high energy stimulation by gamma rays, and X-rays. Deep UV wavelengths are frequently effective in exciting rare-earth phosphor.

The illuminance of trivalent rare-earth ions (Sm^{3+}, Dy^{3+} and Eu^{3+}) in borates have recently piqued interest due to properties such as high stability, wide UV transparency, and low composite temperature, extraordinary optical damage threshold, excellent chemical and thermal stability, and high luminous efficiency [15]. Borates are useful materials because they have a broad transmittance spectrum, an extremely high threshold, a large range of structural types, and excellent optical quality. During UV and blue light excitation, the red fluorescence released by Borate phosphor is extremely important since it is employed to create beneficial and functional applications.

Rare-earth ions are doped in a variety of materials are employed as activator ions for phosphor [16]. The rare-earth ions Sm^{3+}, Eu^{3+}, and Dy^{3+} are regarded as important activator ions for creating radiation in the visible area. Sm^{3+} doped phosphor drew a lot of attention because of the transition from $^4G_{5/2} \rightarrow ^6H_J$, which is employed in optical retention of high-density sensors, underwater communication, and a variety of fluorescence instruments, as well as color display. Samarium's emission spectra exhibit thermostability in the intensity of specific lines, making it suitable for measuring surface temperature on moving turbine blades [17].

1.3 White light emitting diodes (w-LEDs)

When compared to traditional light bulbs, LEDs are more efficient in producing light. White LEDs were not always white LEDs. Instead, a single LED encases bonded red, green, and blue LEDs. Phosphor were used to make the very first white LEDs, which were not confined to one of three LEDs. A complete conversion white LED may be manufactured simply by covering the enclosures with phosphor and placing ultraviolet or violet LEDs inside, however, they are inefficient.

Because of Phosphor's excellent properties such as high efficacy, low potential dissipation, extended lifetime, and low toxicity [18].

In white LEDs, The blue light from the blue LED chip within the photosensitive white LED is captured by the phosphor and converted to yellow light. The phosphor's unconsumed blue light then is transported out. White light may be made by fusing yellow and transmitted blue light having chromaticity coordinates and linked color temperature (CCT) [19].

As a result, a new approach is employed to produce superb full-spectrum white light using tri-color phosphor activated by near-UV (370-410 nm). Because of advantages including intense tolerance to UV chips' color anomaly (cause of phosphor for use in generating white color) and unique color rendering index, it is a flexible and open strategy in attaining maximum white LEDs, but it also results in reduced luminous performance because green and red phosphor possess potent reabsorption in the wavelength range [20].

Rare earth elements as phosphor dopants have been shown to lead to effective photoluminescence in a variety of compounds, allowing their interaction in phosphor-converted LEDs. They feature a low color temperature and a high color rendering [21].

1.4 Photoluminescence (PL)

Photoluminescence is the emission of light by a substance after it has been exposed to light. It's derived from the Latin term luminescence and the Greek suffix photo, which means "light." The light-induced by the absorption of photons is known as photoluminescence. It's a technique in which a particle eats a visible-range photon, excites the electron to a greater excited energy level, and afterward transfers a photon to a lower-energy state, such as an electron.

The experimental method of photoluminescence (PL) is used to characterize semiconductor nanostructures and explore their electrical properties. When the photon energy is larger than the bandgap energy, it is induced by the lighting of the medium. For photoluminescence to occur, wavelengths should be close to the bandgap wavelength. The essential data for device characterization may be derived from the PL spectrum, device temperature, and intensity, which is dependent on irradiation intensity.

In the photoluminescence spectrum of a semiconductor like GaAs, there are several distinct transitions. As a result, the purer GaAs are, the more complicated their PL spectrum will be. For the examination of a photoluminescence spectrum caused by the complex formation of impurities and defects, comprehensive knowledge of the energy levels is necessary. Photoluminescence is a particularly important characterization tool because of the vast amount of data it provides.

PL has a number of benefits, including the ability to create huge amounts of data quickly and easily, the ability to indirectly assess the non-radiative recombination time, and the ability to provide data regarding the system's energy levels and sensitivity. It's a non-destructive method for labeling, stains, chemical markers, and cosmic-ray disclosure on a crystal. Fluorescent lights and LEDs are commonplace, with fluorescent coatings converting short wavelength UV (blue) light to longer wavelength (yellow) light
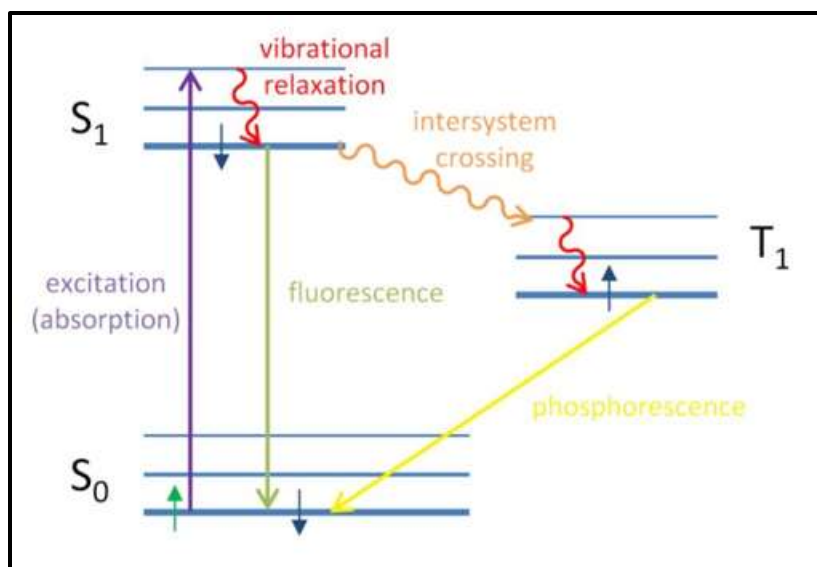
Fig. 1.2. Jablonski diagram of fluorescence and phosphorescence processes

Intersystem crossover (ISC) to the stimulated triplet state is also possible for the molecule (T_1). ISC occurs when molecules have a wide range of spin-orbit coupling, heavy metals like europium and iridium have a high spin-orbit coupling strength. Because the states have different spin multiplicities, the decaying of the T_1 state to the S_0 is a forbidden transition according to angular momentum conservation. However, spin-orbit coupling removes this restriction, making the shift from T_1 to S_1 possible. Because the transition from T_1 to S_0 is 'prohibited,' it takes a long time (microseconds to hundreds of seconds), which is known as phosphorescence as shown in Fig. 1.2.

1.5 Fluorescence and phosphorescence

Fluorescence is photoluminescence that occurs rapidly after material has been photon excited, whilst phosphorescence is long-lasting photoluminescence that occurs after the excitation has ended. In other words, fluorescence is photoluminescence without the necessity for a spin multiplicity change in the radiative transition, whereas phosphorescence is photoluminescence with the need for a spin multiplicity change in the radiative transition.

Molecules with paired electrons are stable, while those with unpaired electrons are exceedingly reactive and volatile. Electrons have a center angular momentum called spin, and the appropriate symmetry of electron spins determines whether an electron belongs in one of two states. When two spins are oriented anti symmetrically, the total spin is zero ($S = 0$), but when they are oriented symmetrically, the total spin is one ($S = 1$). A singlet is an antisymmetric $S = 0$ arrangement of electron spin pairs, while a triplet is three symmetric $S = 1$ permutations of spin pair states.

Whenever the photon is absorbed, one of the pair's electrons is boosted to a higher energy level, and the molecule is said to be in a higher energy state. A molecule's ground energy level is a singlet state (S_0), and the photoexcited state must also be a singlet according to angular momentum conservation (S_1). The decline of the S_1 state to the S_0 state is an authorized transition (because of the identical spin multiplicity), which results in fluorescence on the picosecond to the nanosecond time scale [22].

Mineralogy, gemology, drugs, sensors, and fluorescence affixed at an angle towards the electron, which is then used to produce a 3D image of the sample displayed on a monitor, are some of the practical uses of fluorescence. A conductive adhesive is routinely used to adhere samples tightly to a specimen container. When non-conductive materials are studied by the beam, they build charges, which causes scanning defects and other picture errors, especially in SE imaging mode. Specimens must be good conductors of electricity and flat to prevent the accumulation of electrostatic charges for conventional imaging. Stump metal substance requires just minor preparation aside from conductively connecting to a specimen. A small layer of electrical conductor material is utilized to cover non-conducting components, and then low-vacuum sputter coatings are applied. It is placed on top of the sample. Gold, platinum, tungsten, chromium, graphite, and other conductive materials are utilized for specimen coatings. The morphological features are investigated using the SEM method. It reveals that the particles are micron in size and agglomerated throughout the whole surface [23].

CHAPTER 2

INSTRUMENTATION

CHAPTER 2: INSTRUMENTATION

2.1 Thermal gravimetric analysis (TGA)

TGA stands for thermogravimetric analysis. It is characterization that is done for the sample to study for any mass change concerning the temperature change. Analysis of a material's thermal properties, moisture, and liquid content, and the average concentration of components in a sample are some of its main applications. TGA is primarily used to determine a substance's thermal stability and composition. From the TGA curve, we can tell whether the reaction process is endothermic or exothermic. Weight loss percentage can be calculated too [24].

Fig. 2.1. Thermal gravimetric analysis

2.2 X-ray diffraction (XRD)

X-ray diffraction (XRD) is a significant and broadly utilized material portrayal strategy. With the new improvement in material science innovation and understanding, different new materials are being created, which requires redesigning the current scientific methods to such an extent that arising unpredictable issues can be addressed.
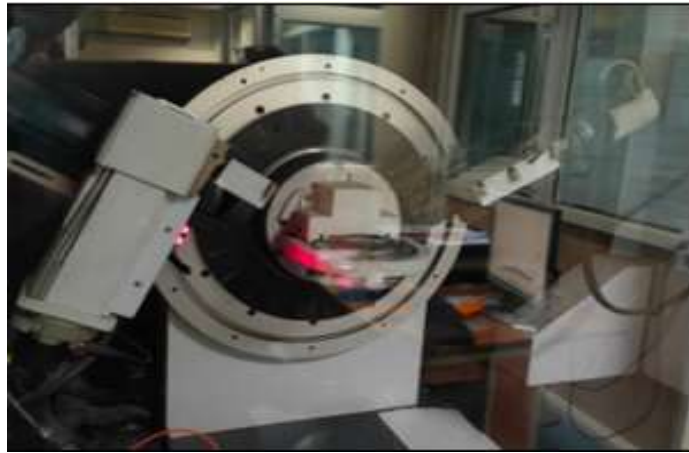
Fig. 2.2. X-ray diffraction

Despite the fact that XRD is a deep-rooted non-disastrous strategy, it actually requires further upgrades in its portrayal capacities, particularly while managing complex mineral designs. The current audit conducts complete conversations on nuclear gem structure, XRD standard, its applications, vulnerability during XRD investigation, and required security safety measures. The future exploration headings, particularly the utilization of man-made reasoning and AI instruments, for working on the adequacy and exactness of the XRD strategy, are talked about for mineral portrayal. The subjects covered incorporate how XRD examples can be used for an intensive comprehension of the translucent construction, size, and direction, separation thickness, stage distinguishing proof, measurement, and change, data about cross-section boundaries, lingering pressure, and strain, and warm development coefficient of materials. This

multitude of significant conversations on XRD examination for mineral portrayal is accumulated in this far-reaching audit, with the goal that it can help subject matter experts and designers in the compound, mining, iron, metallurgy, and steel ventures.

The dynamic scattering of x-ray photons in a periodic lattice by atoms is known as X-ray diffraction. Bragg's law states that scattered monochromatic x-rays in phase produce constructive interference-ray diffraction as shown by equation (2.1) below;

$$n \lambda = 2 \sin \theta \qquad (2.1)$$

A diffractometer records the powder diffraction pattern, and all of the d-values and related energies of the diffraction bands are presented in order to identify an unknown substance. The information is then compared to the traditional line patterns available there in Powder Diffraction File (PDF) databases for various composites [25].

The angle between the incident beam and the perpendicular to the reflective lattice plane, as well as the degree of reflection, the wavelength, the crystal plane spacing, and the angle between the incident beam and the perpendicular to the reflective lattice plane, are all given here. To estimate the value of the spacing by a distance spacings d, the angles of each crystallographic phase are measured.
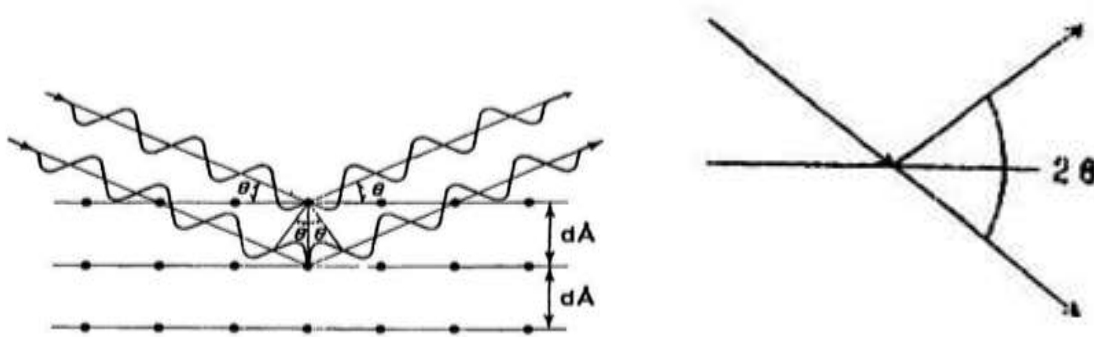

Fig. 2.3. Schematic representation of Bragg's law

To verify the existence of a crystalline structure in either a uniform substance or an inhomogeneous mixture, the existence of the three most intense particular lines from the authorized PDF line model is required. The distinction between conceivable phases can be done by exploring the various characteristic lines in particular subjects [26].

2.1.1 Joint committee on powder diffraction standards (JCPDS)

In 1941, the Joint committee on powder diffraction standards (JCPDS) was established. It maintains the powder diffraction file (PDF), which contains data on powder x-ray diffraction models, particularly relative strengths of notable diffraction peaks in the d-spacings. It is generally used to categorize materials based on x-ray diffraction patterns and is designed for applications. International center for diffraction data is the name given to it currently (ICDD). The PDF of 2019 has distinct sets of material data. Every data set contains diffraction, sample needs, and research and literature data, as well as laboratory, device, crystallographic, and desirable mechanical properties in a conventional graded format. The powder diffraction file databases, educational seminars, clinics, and conferences, as well as the pharmaceutical powder X-ray diffraction symposium, are now all part of it (PXRD) [27].

2.3 Diffuse reflectance spectroscopy (DRS)

Diffuse reflectance spectroscopy is a very well-established approach for examining the spectral features of impenetrable solid materials, based on the principle that certain light reflected from the substance is reflected inwardly and also from the surface (specular reflection) [28].
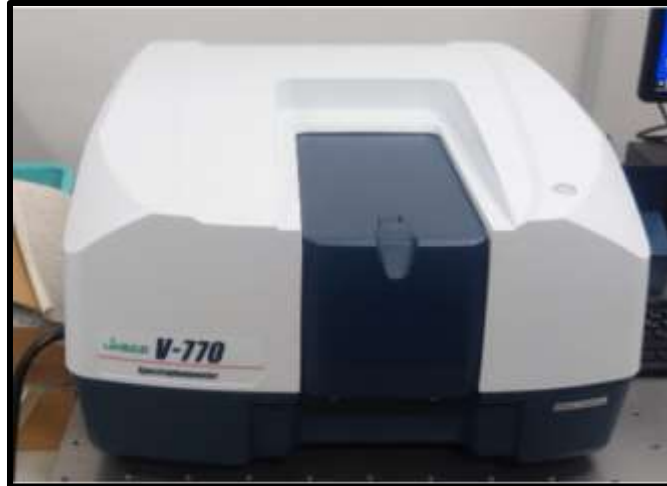
Fig. 2.4. Diffuse Reflectance Spectroscopy

2.4 Fourier infrared transform spectroscopy (FT-IR)

Infrared light is passed through a material by the FT-IR device, with some of it being absorbed but some traveling through. Resulting output at the detector is a spectrum that ranges from 4000 cm-1 to 400 cm-1 and indicates the chemical fingerprint of the material. FT-IR analysis is a good approach for chemical identification since every molecule has its unique spectral fingerprint. The various bands are marked in the transmittance versus wavenumber plot. These bands correspond to the different modes of stretching namely, the symmetric, asymmetric, bending, and so on [29].

Fig. 2.5. Fourier infrared transform spectroscopy

2.5 Scanning electron microscope (SEM)

It's a method for investigating the morphologies of a sample or substance. This is because initially, one has to see whether the data is matching with the reference and peaks and indexes too. Then once observed that the sample material has crystallized well, scanning electron microscopy is performed as discussed above. The electrons are associated with atoms in the specimen, producing a variety of signals, including data about the specimen's surface topography (surface characteristics), morphology (material's appearance), structure, and crystallography (arrangement) [30].

Fig. 2.6. Scanning electron microscope

The electron beam studies the specimen in a raster approach in scanning electron microscopy. The electrons at the apex of the column come from the electron source. These are released when the thermal energy exceeds the work function of the reference element. The anode activates and excites them subsequently (positively charged). To defend it from pollution, vibrations, and noise, the whole electron column must be placed under a vacuum. The vacuum allows the operator to receive a high-resolution image while still increasing the detector's electron gathering capability. The electrons' course is controlled by Lenses. Two electromagnetic lenses are used: The beam is collected by the condenser lens, which will then be converted by the objective lens before striking the specimen. The intensity of the electron beam

is governed by the condenser lens, while the objective lens concentrates the beam toward the specimen [31].

2.6 Photoluminescence (PL) spectroscopy

Light is focused onto a specimen in photoluminescence spectroscopy, here it is absorbed and photosensitizer may occur, leading in the emission of photoluminescence. For room and lowest temperature spatially resolved micro-PL, a concentrated laser beam offers a chromatic aberration spot width of the order of 1 m. A CCD camera captures the spectrum for every investigated place when scanning the sample. When employing luminous materials, examine the emission, quantum yield, luminescence energy transfer, Diffuse duration, chemical/physical durability, and other factors [32].

Fig.2.7. Photoluminescence spectroscopy

CHAPTER 3

EXPERIMENTAL PROCEDURE

CHAPTER 3: EXPERIMENTAL PROCEDURE

3.1 Synthesis: Solid state reaction method

This is the most popular process for preparing phosphor for use in a variety of applications. Starting with diverse solid ingredients necessary for the final product, the preparation procedure is used. A high temperature of around 1000-1500°C is given for a short length of time to allow the reactions to occur. Solid reactants are employed in the production of phosphor or any crystalline chemical. The chemical reactants utilized in it are determined by their practicality, as well as some reaction parameters and the ultimate product. The reactants are combined after they have been weighted according to their stoichiometric ratios in the chemical equation. Acetone or alcohol are examples of volatile organic liquids that are added to the mixture in sufficient quantities to ensure that almost all of the reactants are evenly distributed. A paste-like mixture is generated, which is extensively ground until the organic solvent volatilizes and evaporates entirely, which takes around 10-15 minutes, resulting in a powder-like substance. In a furnace, a subsequent reaction occurs at high temperatures. The real advantage of a solid-state reaction is that the final product is pure and has the qualities that are sought. This process produces no waste or hazardous material and is ecologically friendly.

3.2 Sample preparation: $K_5BiMo_4O_{16}$

Stoichiometric ratios are calculated via chemical methods. The masses of the reactants K_2CO_3, Bi_2CO_3, and MoO_3 are calculated based on the concept of equal reactant and product sides. In this scenario, 3 g of KBM was required. The KBM sample synthesis procedure was to take an agate mortar, all of the calculated reactants are put, and just enough ethanol is added to mix them all. To produce a powder composition, the paste is pounded for roughly an hour in a mortar. In a muffle furnace, the powder is

sintered in a silica crucible. Three different temperatures were used to sinter the KBM samples which are 800, 900, and 1000 °C.

3.3 Analysis of sample

The KBM phosphor are manufactured using varying mol percent values of Eu^{3+} doping. An X-ray diffractometer was utilized to examine the crystalline properties of these materials (Bruker: model D8 advance). It uses nickel filtered $CuK\alpha$ (=1.541 A°) to scan the sample at an angle of 2 ranging from 20° to 60°. With the help of a JASCO spectrophotometer, bandgap studies are carried out (Model no. V-770). The Perkin Elmer Spectrum Two FT-IR spectrometer was utilized to explore the bonding modes in the crystal lattice in the region of 400 to 1600 cm^{-1}. The morphological findings were investigated utilizing a JEOL 7610F Plus scanning electron microscope. The photoluminescence properties were measured using a Shimadzu RF-5301 PC Spectro fluorophotometer. The excitation and emission spectra were captured using a JASCO FP-8300 fluorescence spectrophotometer and an excitation source (Xenon lamp).

CHAPTER 4

RESULTS AND DISCUSSION

CHAPTER 4: RESULTS AND DISCUSSION

4.1 Structural studies

X-ray Diffraction studies for undoped and Eu^{3+} doped $K_5BiMo_4O_{16}$ phosphor were carried out at different temperatures as shown in Fig. 4.1.(a) for examining phase purity. The XRD was also carried out for 1.0 mol% doping of Eu^{3+} in KBM, depicted by Fig. 4.1.(b). The XRD patterns clearly depicted sharp and single peaks. This shows that the sample has crystallized well suggesting the formation of a single-phase polycrystalline nature. The pure phase begins at 800°C. The experimental data matches close to the known data, that is, the JCPDS (29-0986) file.
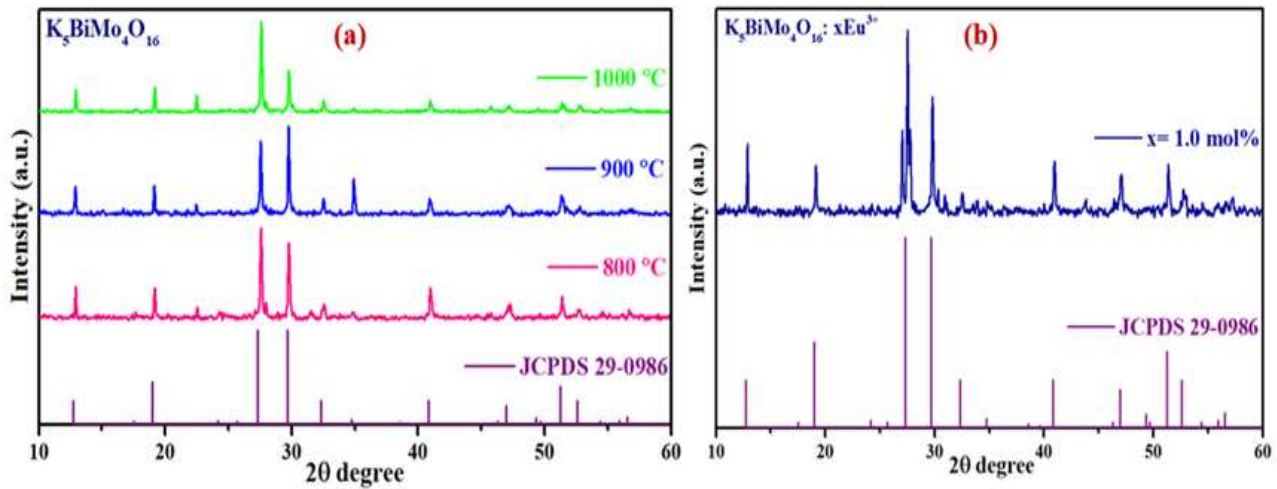
Fig. 4.1. XRD patterns of KBM phosphor at (a) different sintering temperatures 800, 900, and 1000 °C (b) 1.0 mol% concentration Eu^{3+} doped KBM phosphor

The Crystallite size has been calculated with the help of the XRD pattern for $K_5BiMo_4O_{16}$. This is done using the Debye-Scherrer formula for determining the crystallite size which is stated as follows;

$$\text{Crystallite size } (D) = K\lambda/\beta cos\theta \qquad (4.1)$$

The crystallite size for doped and undoped Eu^{3+} doped KBM phosphor was calculated to be 0.44 and 0.45 μm, respectively.

4.2 Diffuse reflectance spectroscopy

The optical band gap for undoped and Eu^{3+} doped KBM phosphor was evaluated making use of DRS in the wavelength range of 200 – 600 nm at RT (Fig. 4.2). To determine the optical band gap, the diffuse reflectance was translated into the Kubelka Munk (K-M) function, as shown in the equation below:

$$F(R) = \frac{(1-R)^2}{2R} = \frac{K}{S} \qquad (4.2)$$

where R is the sample reflectance and K and S are the scattering and absorption constants. As demonstrated in the equation, the linear absorption constant in the Tauc equation has a relationship with bandgap energy (E_g):

$$\alpha h\upsilon = A(h\upsilon - E_g)^n \qquad (4.3)$$

where h is light energy, A is the proportionality constant, and n is the electronic transition with values 1/2, 2, 3/2, and 3, expressing the authorized direct, allowed indirect, banned direct, and forbidden indirect bandgaps with associated electronic transition values.

The band gap was calculated by projecting a linear fit line towards the x-axis. The displayed graph shows the direct permitted bandgap for undoped and 1.0 mol % of Eu^{3+} doped KBM samples with values of 3.60 eV and 3.58 eV, respectively.
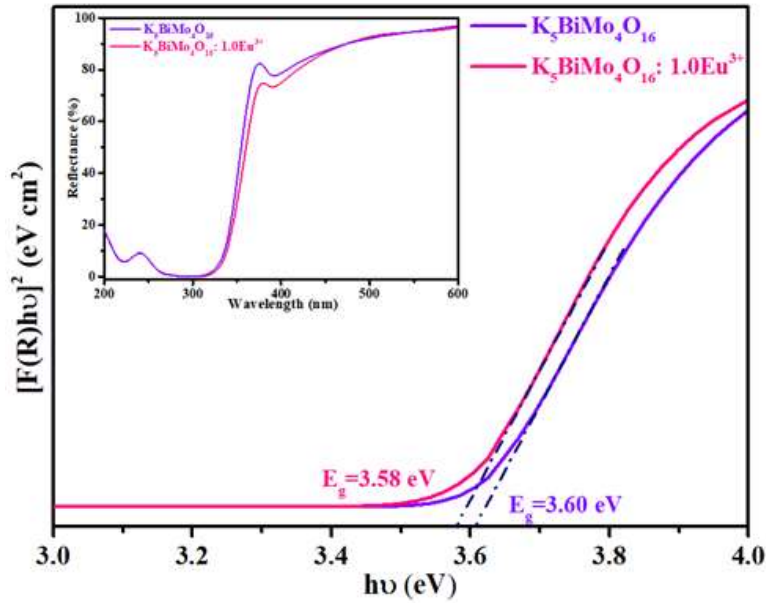
Fig. 4.2 Optical bandgap energy of undoped and 1.0Eu^{3+} doped KBM at 800 °C (Inset: UV diffuse reflectance spectra of undoped and 1.0Eu^{3+} doped KBM at 800 °C)

4.3 Fourier transform infrared spectroscopy

The Fourier Transform Infrared Spectroscopy highlights the sample's critical characteristics, such as the bond production and current functional groups in the synthesized Eu^{3+} doped KBM phosphor. The Fourier Transform Infrared Spectroscopy highlights the sample's critical characteristics, such as the bond production and current functional groups in the synthesized Eu^{3+} doped KBM phosphor. The Fourier Transform Infrared spectroscopy of the K$_5$BiMo$_4$O$_{16}$ phosphor is shown in Fig. 4.3. The transmittance versus wavenumber diagram shows the various bands. These bands represent various stretching modes, such as symmetric, asymmetric, bending, and so on. They have also been tabulated in the table below Table 4.1.
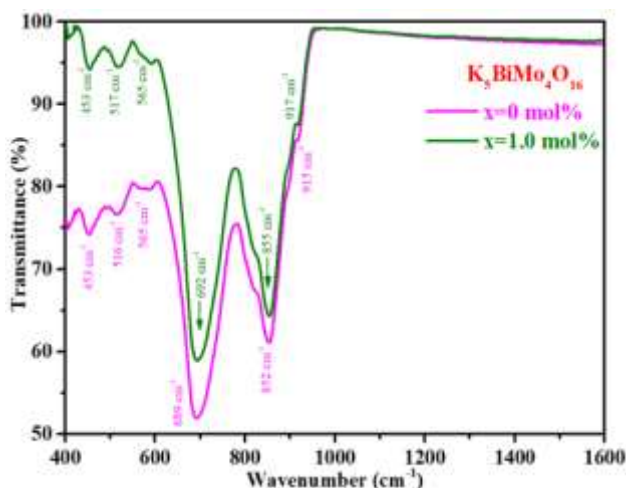
Fig. 4.3. FT-IR patterns of undoped and 1.0 mol% Eu^{3+} doped $K_5BiMo_4O_{16}$ phosphor

Table 4.1. Bands of KBM samples corresponding to the different modes of stretching

Bands (in cm^{-1})	Modes	Bonds
915	Symmetric stretching	$Mo-O_4$
852	Asymmetric stretching vibrational	$Mo-O$
689	Symmetric scissor and stretching vibrations	$Bi-O_2$
453	Bending modes	$Bi-O_3$
516 and 565	Rocking Vibration	$Bi-O$

4.4 Morphological studies

Scanning electron microscopy was carried out using High-resolution field emission scanning electron microscope (HR-FE-SEM) 7610F Plus-JEOL. The shape, size, and morphology of the KBM phosphor were studied carefully. It can be observed that there are no significant changes in the morphology of the sample when Eu^{3+} is doped in KBM.
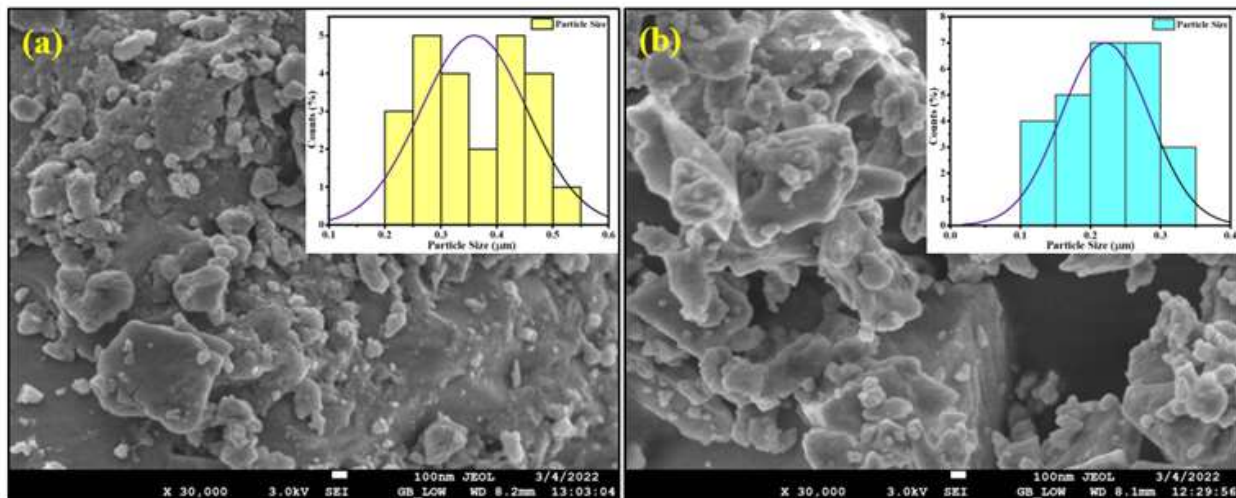
33

Fig. 4.4. SEM micrographs of KBM Phosphor

The particles are in micro range and the morphology is non-uniform. The average particle size lies in the range of 0.2 to 0.6 μm, inset of the Fig.4.4. which shows the particle size distribution of undoped and KBM: $1.0Eu^{3+}$ phosphor.

4.5 Photoluminescence spectra

4.5.1 Excitation spectra

The excitation spectra of 1.0 mol% Eu^{3+} doped KBM phosphor were recorded by fixing an emission wavelength of 574 nm. The two most intense peaks were found in the near UV region at 392 nm and the blue region at 464 nm wavelength. Various other peaks were located at 360, 380, 392, 413, 464, and 485 nm in the excitation spectra due to f-f transitions of Eu^{3+} ions. This is shown in our intensity versus wavelength plot below in Fig. 4.5. (a).

4.5.2 Emission spectra

The Photoluminescence Emission (PL) spectra of 1.0 mol% Eu^{3+} doped KBM phosphor were recorded by fixing an emission wavelength of 574 nm. The PL spectra highlight peaks located at 578, 588, 612,

657, and 704 nm. The most prominent peak in the spectra appeared at 612 nm owing to the $^5D_0{\rightarrow}^7F_2$ transition. The emission plot is shown below in Fig. 4.5.(b).
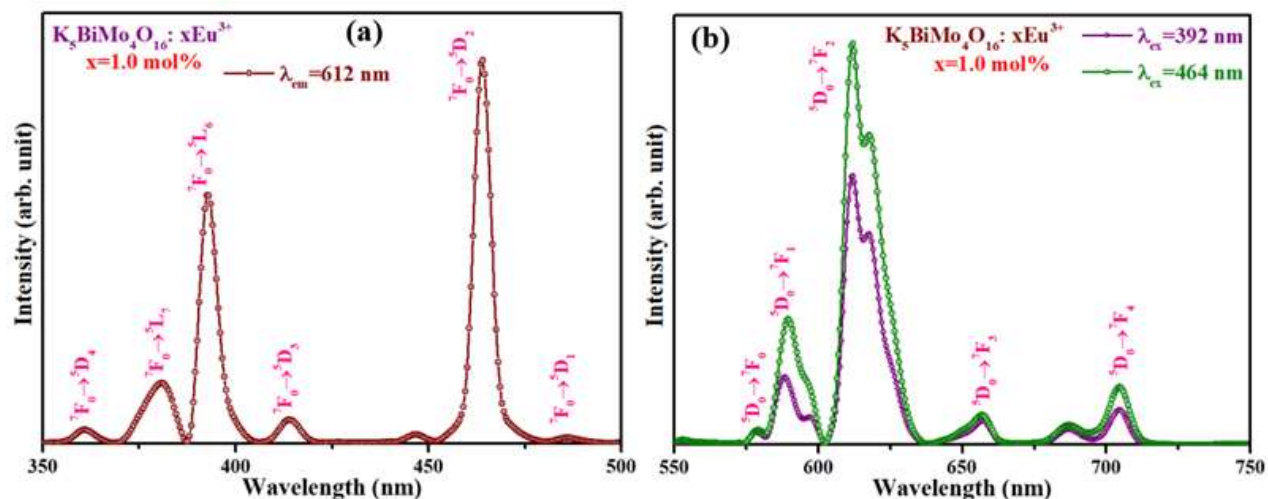

Fig. 4.5. (a) PLE spectrum of 1.0 mol% of Eu^{3+} doped KBM phosphor at 612 nm emission wavelength (b) Emission spectra of 1.0 mol% of Eu^{3+} doped KBM phosphor at two different excitation wavelengths

4.6 Color chromaticity diagram for KBM

As per the following plot (Fig. 5.6), (0.657, 0.342) and (0.655, 0.344) are found to be CIE color coordinates for 1.0 mol% Eu^{3+} doped KBM under excitation wavelengths of 392 and 464 nm respectively. When excited with n-UV and blue light, the CIE chromaticity coordinates are in the red area. The color (CCT) values of as-synthesized phosphor have been determined using McCamy's polynomial formula:

$$CCT = -437n^3 + 3601n^2 - 6861n + 5514.3 \tag{4.4}$$

where n denotes the inverse slope line, which is equal to the ratio of $(x-x_e)$ to $(y-y_e)$, and $x_e=0.332$ and $y_e=0.186$ denote the convergence center.
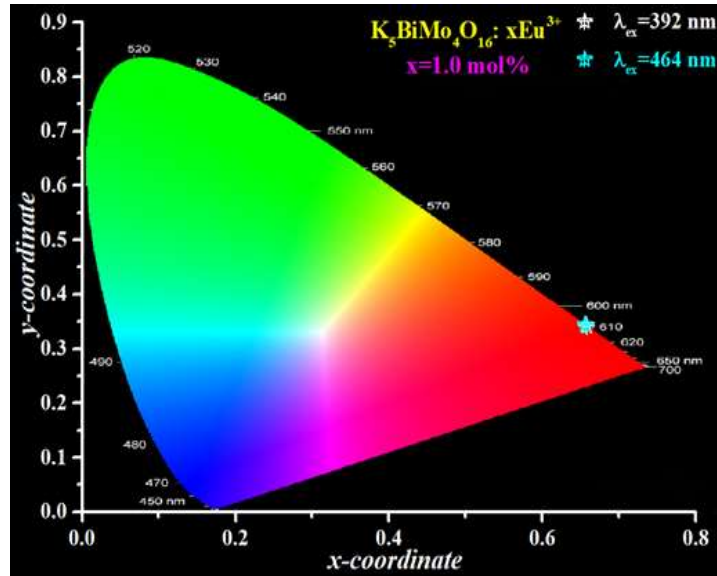
Fig. 4.6. CIE chromaticity diagram of 1.0 mol% of Eu^{3+} doped KBM phosphor under excitation wavelengths of λ_{ex}=392 nm and λ_{ex}=464 nm.

Under 392 and 464 nm excitation wavelengths, the estimated CCT values for 1.0 mol % Eu^{3+} doped KBM phosphor are 2901 and 2801 K, respectively. Phosphor with a CCT value less than 5000 K are better for warm light applications, while those with values higher than 5000 K are better for cool light applications. As a result, the CCT values for 1.0 mol % Eu^{3+} doped KBM phosphor were less than 5000 K, indicating that it may be used in warm w-LED applications.

CHAPTER 5

CONCLUSIONS

CHAPTER 5: CONCLUSIONS

High-quality $K_5BiMo_4O_{16}$:Eu^{3+} phosphor have been synthesized by the conventional solid-state reaction technique and characterized for their structural and photoluminescence properties. The powder XRD indicated that phosphor crystallized well and are single phase. SEM micrographs have depicted the inhomogeneous morphology of these phosphor which indicated KBM to be submicron-sized and agglomerated all over the surface. Their luminescence properties have been studied for both excitation and emission spectra respectively. KBM shows the intense red emission at 612 nm excited under n-UV and blue light. The color coordinates obtained from emission spectra are found to lie in red region for KBM. The CIE chromaticity coordinates for this phosphor represent red emission of the as-synthesized phosphor, which indicates that it can be used in cost-effective phosphor-converted white light-emitting diodes (pc-wLED).

CHAPTER 6

SCOPE OF WORK

CHAPTER 6: SCOPE OF WORK

The recent work has been done by doping Dysprosium (Dy^{3+}) and Europium (Eu^{3+}) into NBB and KBM host materials respectively which have made them an effective and high-quality phosphor which can be used in low-cost developed phosphor-converted white light-emitting diodes (pc-wLEDs). They can also be employed for similar opto-electronic applications. Firstly, the luminescent properties of these phosphor can be enhanced via co-doping with other suitable rare-earth ions (RE) such as yttrium (Y^{3+}), samarium (Sm^{3+}), gadolinium (Gd^{3+}), terbium (Tb^{3+}), and lutetium (Lu^{3+}), etc. This is because RE ions co-doped in specific regions of host matrix could enable a new generation of quantum integrated photonic devices.

The present phosphor has been synthesized by the conventional solid-state reaction technique and characterized for their structural and photoluminescence properties. So, another synthesis method such as sol-gel method can be explored to improve the particle morphology and reduce the particle size. The sol-gel combustion method employs a hybrid of the sol-gel and combustion processes, with nitrates as metal precursors. The metal oxides that are generated go through numerous processes in the Sol–gel approach. First, the metal nitrate is rapidly hydrolysed; second, the metal hydroxide solution is condensed to create gels; and finally, xerogel is formed following the evaporation process, which is then combusted at a high temperature. The resulting compound is a black fluffy structure that is sintered at various temperatures. This method may be explored to improve the luminescence properties of the as-prepared phosphor.

The utility of these phosphor can not only be applied for wLEDs but also is extended for versatile applications such as fingerprint sensing and thermal sensing, bio-imaging, etc. In a nutshell, the prototype w-LEDs can be fabricated using the optimized phosphor for the above-mentioned applications.

REFERENCES

[1]   S. Pradhan, H. Kaur, M. Jayasimhadri, Photoluminescence and thermal sensing properties of Er^{3+} doped silicate-based phosphor for multifunctional optoelectronic device applications, Ceram. Int. 47 (2021) 27694–27701.

[2]   Z. Li, X. Geng, Y. Wang, Y. Chen, Synthesis and luminescence properties of $NaBaPO_4:Tm^{3+,}Dy^{3+}$ white-light emitting phosphor with enhanced brightness by Li^+ co-doping, J. Lumin. 240 (2021).

[3]   G.R. Dillip, G.B. Kumar, V.R. Bandi, M. Hareesh, B. Deva Prasad Raju, S.W. Joo, L.K. Bharat, J.S. Yu, Versatile host-sensitized white light emission in a single-component $K_3ZnB_5O_{10}: Dy^{3+}$ phosphor for ultraviolet converted light-emitting diodes, J. Alloys Compd. 699 (2017) 1108–1117.

[4]   T.S. Sreena, P.P. Rao, A.K.V. Raj, T.R.A. Thara, Narrow-band red-emitting phosphor, $Gd_3Zn_2Nb_3O_{14}: Eu^{3+}$ with high color purity for phosphor-converted white light emitting diodes, J. Alloys Compd. 751 (2018) 148–158.

[5]   H. Kaur, M. Jayasimhadri, Color tunable photoluminescence properties in Eu^{3+} doped calcium bismuth vanadate phosphor for luminescent devices, Ceram. Int. 45 (2019) 15385–15393.

[6]   Q. Zhang, X. Wang, Y. Wang, Design of a broadband cyan-emitting phosphor with robust thermal stability for high-power WLED application J. Alloys Compd. 886 (2021) 161217.

[7]   L. Jun, X. Shuping, G. Shiyang, FT-IR and Raman spectroscopic study of hydrated borates, Spectrochim. Acta A Mol. Biomol. Spectrosc. SPECTROCHIM ACTA A. 51 (1995) 519-532.

[8]   C.S. Lim, A.S. Aleksandrovsky, M.S. Molokeev, A.S. Oreshonkov, D.A. Ikonnikov, V. v. Atuchin, Triple molybdate scheelite-type upconversion phosphor $NaCaLa(MoO_4)_3:Er^{3+}/Yb^{3+}$: Structural and spectroscopic properties, Dalton Trans. 45 (2016) 15541–15551.

[9]   S. Das, A. Amarnath Reddy, S. Surendra Babu, G. Vijaya Prakash, Controllable white light emission from Dy^{3+}-Eu^{3+} co-doped $KCaBO_3$ phosphor, J. Mater. Sci. 46 (2011) 7770–7775.

[10] B. Han, Y. Dai, J. Zhang, B. Liu, H. Shi, Development of near-ultraviolet-excitable single-phase white-light-emitting phosphor $KBaY(BO_3)_2$:Ce^{3+} ,Dy^{3+} for phosphor-converted white light-emitting-diodes, Ceram. Int. 44 (2018) 14803–14810.

[11] M. Jayachandiran, S.M.M. Kennedy, Synthesis and optical properties of $Ba_3Bi_2(PO_4)_4$: Dy^{3+} phosphor for white light emitting diodes, Journal of Alloys and Compounds. 775 (2019) 353–359.

[12] Y. Shi, Z. Yang, W. Wang, G. Zhu, Y. Wang, Novel red phosphor Na_2CaSiO_4:Eu^{3+} for light-emitting diodes, Mater. Res. Bull. 46 (2011) 1148–1150.

[13] X. Lei, G. Li, M. Zeng, B. Zhou, Z. Yuan, Y. Hu, H. Gu, Y. Li, W. Chen, Europium-doped $NaBaB_9O_{15}$ phosphor with controllable blue/red dual-band emissions through self-reduction for plant growth LEDs, J. Lumin. 237 (2021) 118166.

[14] C.H. Lin, C.H. Huang, Y.M. Pai, C.F. Lee, C.C. Lin, C.W. Sun, C.H. Chen, C.W. Sher, H.C. Kuo, Novel method for estimating phosphor conversion efficiency of light-emitting diodes, Crystals (Basel). 8 (2018) 120442.

[15] H. Kaur, M. Jayasimhadri, Spectroscopic and color tunable studies in Dy^{3+}/Eu^{3+}co-doped calcium-bismuth-vanadate phosphor for lighting applications, Solid State Sci. 122 (2021) 106776.

[16] M. Sahu, N. Phatak, M.K. Saxena, Exploring color tunable emission characteristics of Eu^{3+}-doped $La_2(MoO_4)_3$ phosphor in the glass-ceramic form, RSC Adv. 11 (2021) 17488–17497.

[17] L. Wang, X. Guo, Q. Song, J. Li, X. Wang, N. Wang, Y. Li, Y. Han, G. Jia, Multicolor barium molybdate phosphor doped with Re^{3+} (Re = Eu, Sm, Tb, Dy) via solid-state method: Synthesis and characterizations, Modern Physics Letters B. 32 (2018).

[18]   T. Sakthivel, G. Annadurai, R. Vijayakumar, X. Huang, Synthesis, luminescence properties and thermal stability of Eu^{3+}- activated $Na_2Y_2B_2O_7$ red phosphor excited by near-UV light for pc-WLEDs, J. Lumin. 205 (2019) 129–135.

[19]   C. Dou, Z. Wang, Y. Yin, C. Liu, F. Zheng, S. Sun, B. Teng, J. Li, D. Zhong, Realization of non-rare earth doped blue-emitting phosphor $Ba_2Y_5B_5O_{17}$: Sb by selective site excitation, and its application in n-UV excited wLEDs, J. Lumin. 239 (2021) 118326.

[20]   J. Grigorjevaite, A. Katelnikovas, Synthesis and optical properties investigation of blue-excitable red-emitting $K_2Bi(PO_4)(MoO_4):Pr^{3+}$ powders, J. Mater. Res. Technol. 9 (2020) 15779–15787.

[21]   Y. Zhai, W. Zhang, Y. Yin, J. Wang, C. Hu, X. Li, Facile hydrothermal synthesis and luminescent properties of monodisperse ellipsoid-like $NaLa(MoO_4)_2:Sm^{3+}$ red-emitting phosphor, J. Mater. Sci.: Mater. Electron. 27 (2016) 9690–9698.

[22]   B. Valeur, M.N. Berberan-Santos, A brief history of fluorescence and phosphorescence before the emergence of quantum theory, J. Chem. Educ. 88 (2011) 731–738.

[23]   Fluorescence and Phosphorescence - Chemistry LibreTexts, (n.d.).

[24]   P. Basu, Analytical techniques, Biomass Gasification, Pyrolysis and Torrefaction: Practical Design and Theory. (2018) 479–495.

[25]   F. Sima, C. Ristoscu, L. Duta, O. Gallet, K. Anselme, I.N. Mihailescu, Laser thin films deposition and characterization for biomedical applications, Laser Surface Modification of Biomaterials: Techniques and Applications. (2016) 77–125

[26]   N. Fleck, H. Amli, V. Dhanak, W. Ahmed, Characterization techniques in energy generation and storage, Emerging Nanotechnologies for Renewable Energy. (2021) 259–285.

[27] R. Jenkins, T.G. Fawcett, D.K. Smith, J.W. Visser, M.C. Morris, L.K. Frevel, JCPDS — International Centre for Diffraction Data Sample Preparation Methods in X-Ray Powder Diffraction, Powder Diffraction. 1 (1986) 51–63.

[28] A.J. Moy, J.W. Tunnell, Diffuse Reflectance Spectroscopy and Imaging, Imaging in Dermatology. (2016) 203–215.

[29] N.R.R. Anbusagar, K. Palanikumar, A. Ponshanmugakumar, Preparation and properties of nanopolymer advanced composites: A review, Polymer-Based Nanocomposites for Energy and Environmental Applications: A Volume in Woodhead Publishing Series in Composites Science and Engineering. (2018) 28–73.

[30] N.C.I.S. Furuvik, L. Wang, R. Jaiswal, R. Thapa, M.S. Eikeland, B.M.E. Moldestad, Experimental study and SEM-EDS analysis of agglomerates from gasification of biomass in fluidized beds, Energy. 252 (2022) 124034.

[31] L. Gómez, I. Martínez, M. v. Navarro, T. García, R. Murillo, Sorption-enhanced CO and CO_2 methanation (SEM) for the production of high purity methane, Chem. Eng. J. 440 (2022) 135842.

[32] The Current Situation in Ultra-Precision Technology – Silicon Single Crystals as an Example, Advances in CMP Polishing Technologies. (2012) 15–111.

PLAGIARISM REPORT

turnitin

Similarity Report ID: oid:27535:17094107

PAPER NAME

Plag.docx

AUTHOR

Divyanshi Tanisha

WORD COUNT

5762 Words

CHARACTER COUNT

32290 Characters

PAGE COUNT

36 Pages

FILE SIZE

2.9MB

SUBMISSION DATE

May 11, 2022 8:37 AM GMT+5:30

REPORT DATE

May 11, 2022 8:38 AM GMT+5:30

● **3% Overall Similarity**

The combined total of all matches, including overlapping sources, for each database.

- 2% Internet database
- Crossref database
- 2% Submitted Works database

- 1% Publications database
- Crossref Posted Content database

● **Excluded from Similarity Report**

- Small Matches (Less then 10 words)
- Manually excluded sources

DELHI TECHNOLOGICAL UNIVERSITY

(FORMERLY Delhi College of Engineering)

Bawana Road, Delhi-110042

PUBLISHED PAPER PROOF

Structural and spectroscopic studies of Eu^{3+} activated potassium bismuth molybdate phosphor for optoelectronic device applications

Divyanshi Nagpal, Tanisha Bhadauria, M. Jayasimhadri *

Luminescent Materials Research Lab, Department of Applied Physics, Delhi Technological University, Bawana Road, Delhi 110 042, India

ARTICLE INFO

ABSTRACT

Red emitting Eu^{3+} activated K$_3$BiMo$_4$O$_{16}$ (KBM: Eu^{3+}) phosphor has been synthesized via high temperature solid state reaction route and explored via investigating various structural and spectroscopic properties. The phase purity of the as-synthesized KBM samples have been analysed through X-ray diffraction technique. Morphological properties have been analysed through SEM images and the vibration modes have been identified in KBM crystal using Fourier Transform Infrared (FT-IR) spectroscopy. The luminescence spectrum of KBM: Eu^{3+} phosphor indicates the characteristic peaks of Eu^{3+} positioned at 578, 588, 612, 657 and 704 nm under 392 and 464 nm excitation wavelength. The color coordinates of KBM: Eu^{3+} phosphor excited with 392 and 464 nm wavelength are (0.657, 0.342) and (0.655, 0.344) located in red region. Based on the above-mentioned characteristics, KBM: Eu^{3+} phosphor may be a potential candidate to utilize in optoelectronic applications such wLEDs and solar cells.

1. Introduction

Among all conventional lighting sources, phosphor converted white LEDs (pc-wLEDs) render great advantages as they possess remarkable energy efficiency, good thermal stability, compact in size, high brightness, long operating lifetime, higher colour rendering index (CRI) and eco-friendliness etc [1–4]. However, pc-wLEDs also have certain issues such as low efficiency, halo effect, low color rendering index (CRI), and high color correlated temperature (CCT) value owing to deficient of red component in the crystal matrix to produce efficient white light [5]. Henceforth, the researchers and scientists are oriented to develop promising red emitting phosphor to achieve intense white light based on pc-wLEDs [6,7]. Recently, pc-wLEDs have attracted much interest in which red/green/blue phosphors excited with UV or near UV (n-UV) radiation emitting LED chip to produce white light [8].

Due to distinctive features of f-f intra configurational transitions, a trivalent rare earth (RE) ion such as Eu^{3+} doped appropriate host lattice can be used as a promising red emitting phosphor [9].

Europium ion doped phosphor has been acquiring interest due to its characteristic transitions, to employ in various applications such as display panels, lasers, solar cell and several optoelectronic devices. Moreover, appropriate host and dopant ions are required to attain qualitative luminescence. Various phosphor materials such as silicates, borates, aluminates, molybdates, vandates etc., have been explored due to the fact that they possess large band gap, high chemical and thermal stability. In this regard, alkali based bismuth molybdate hosts are presently being researched as a potential material for luminescent ions [10,11]. Since, the ionic radius of Bi^{3+} is near to the ionic radii of lanthanides, so that the bismuth containing compound can be easily doped with luminous rare earth ions [12].

In the present study, Eu^{3+} doped K$_3$BiMo$_4$O$_{16}$ (KBM) molybdate phosphor has been synthesized via solid state reaction route and explored its capability as luminescent material for optoelectronic device applications. In this direction, 1.0 mol% Eu^{3+} doped KBM phosphor has been investigated for its structural, morphological and luminescence behaviour in detail. The findings achieved in the current study endorses that the obtained red emitting KBM: 1.0Eu^{3+} phosphor could be an excellent candidate for w-LEDs and solar cell applications.

* Corresponding author.
E-mail address: jayashrie@dtu.ac.in (M. Jayasimhadri).

ACCEPTANCE PROOF

13th INTERNATIONAL CONFERENCE ON
Materials Processing and Characterization

ACCEPTANCE LETTER

E-mail:icmpc-hyd@griet.ac.in   Phone: +91-9959870237

Conveners
Dr. Swadesh Kumar Singh, Professor, GRIET Hyderabad
Dr. Chetan P Nikhare The Pennsylvania State University, USA
Dr. Asma Perveen, Assistant Professor, Department of Mechanical Engineering, Nazarbayev University, Kazakhstan
Dr Julfikar Haider, Manchester Metropolitan University, United Kingdom
Dr. Rajesh Purohit, Professor, MANIT Bhopal

Organising secretary
Dr. B Tarya, Associate Professor, GRIET Hyderabad, India
Dr. R. S. Rana, Associate Professor, MANIT Bhopal
Dr. Manish Vishwakarma, Assistant Professor, MANIT Bhopal

Advisory Committee
Dr. J.W. Yoon, Deakin University, Australia
Dr. Jaros Law Darlich, Michigan Technological University, USA
Dr. Bernard Rolfe, Deakin University, Australia
Dr. Fan Gang Tseng, Taiwan
Dr. Stephen Bigger, Victoria University, Melbourne, Australia
Dr. Vickita Krishna, Deputy Director, VSSC, Trivandrum
Prof. Diogo Mariano Neto, University of Coimbra, Portugal
Dr. S.L. Mannan, Former Scientist, IGCAR, Consultant, GTRE
Prof. K. Narayanan, IIT Bombay
Dr. V. Pancholi, IIT Roorkee
Dr. K. S. Suresh, IIT Roorkee
Dr. A.K. Singh, Scientist, DMRL, Hyderabad
Dr. Sunil Pandey, Director & Vice-Chancellor
Dr. N. Eswara Prasad, Regional Director, RCMI, CEMILAC, Hyderabad
Dr. M. Manohar, VSSC, Trivandrum
Dr. T.K. Nandy, Scientist, DMRL, Hyderabad
Dr. I.V. Singh, IIT Roorkee
Dr. T. Raghu, Scientist, DMRL, Hyderabad
Dr. C. Vanitha, NIT Warangal
Dr. G. Padmanabham, Associate Director, ARCI, Hyderabad
Dr. D. Ravi Kumar, IIT Delhi
Dr. Ramesh Kumar, DRDL, Hyderabad
Dr. Ravi Kumar N V, IIT Madras
Dr. Manoj Kumar Gupta, Scientist, IPR, Gujrat
Dr. A.K. Gupta, BITS Pilani, Hyderabad
Dr. S.K. Panda, IIT Kharagpur
Dr. S.D. Kore, IIIT Guwahati
Dr. Balu Naik, JNTU, Hyderabad
Dr.Alok Kanjilal, Professor, Shiv Nadar University, Delhi-NCR
Dr Kushavendra Chaudhary, Principal, SISTEC, Bhopal
Dr. M. M. Malik, Professor, MANIT Bhopal
Dr. S. P. S. Rajput, Professor, MANIT Bhopal

Date:17/04/2022

To

Tanisha Bhadauria

Luminescent Materials Research Lab, Department of Applied Physics, Delhi Technological University, Bawana Road, Delhi-110 042, India

Dear Sir

It is our pleasure to inform you that your paper entitled **"Structural and spectroscopic studies of Eu3+ activated potassium bismuth molybdate phosphor for optoelectronic device applications "** (MATPR-D-22-02961) has been accepted for oral paper presentation at ICMPC-2022 and publication in Materials Today: Proceedings

You are requested to send the dully filled registration form and copyright form along with Demand Draft or bank transaction receipt. The program for the upcoming conference will be loaded on the website as soon as it is finalized. We are looking forward to your participation at the conference.

Thanks and Regards,

Dr. Swadesh Kumar Singh,
GRIET, Hyderabad.

REGISTERATION PROOF

13th INTERNATIONAL CONFERENCE ON
Materials Processing and Characterization
@ GRIET, Hyderabad   22nd-24th April 2022

REGISTRATION FORM

PAPER ID: 823

Full Name: Tanisha Bhadauria

Designation: Student

Organization & Address: Delhi Technological University, Bawana Rd Shahbad Daulatpur Village, Rohini, New Delhi, Delhi 110042

Mobile: 7007097081 **Phone (o):**

E-mail: tanishabhadauria_2k20mscphy30@dtu.ac.in

Amount paid: AMPT (Taylor and Francis) : Rs 15000 / USD 250

AIP Conference proceedings : Rs 9000/ USD 175

✓ **Materials Today: Proceedings: 9000/**

Name of the Bank: State Bank of India

Name of the account holder: Tanisha Bhadauria

Date of the transaction: 08 April, 2022

Online Transaction number: IMPS001199073471

Registration Category: Educational Institution

Signature with Date

Correspondence Address:
ICMPC-2022
GOKARAJU RANGARAJU INSTITUTE OF ENGINEERING &
TECHNOLOGY BACHUPALLY, HYDERABAD-500090 TELANGANA, INDIA.
PHONE.NO: 091-9959870257
E-mail: icmpc-hyd@griet.ac.in